

Supporting Information

Impact of Polymer Modifier on Directing Non-classical Crystallization Pathway of TS-1 Zeolite: Accelerating Nucleation and Enriching Active Sites

Jiani Zhang,^a Risheng Bai,^a Yida Zhou,^a Ziyi Chen,^b Peng Zhang,^b Jiyang Li*^a and Jihong Yu*^a

^aState Key Laboratory of Inorganic Synthesis and Preparative Chemistry, College of Chemistry, Jilin University Changchun 130012, China

E-mail: jihong@jlu.edu.cn, lijyang@jlu.edu.cn

^bDepartment of Chemistry, Dalhousie University, Halifax, Nova Scotia, Canada, B4H4R2

E-mail: peng.zhang@dal.ca

Table of contents	Page
Experimental section	S5
Characterizations	S6
Catalytic tests	S7
Supplementary Figures	S9
Supplementary Tables	S45

List of Supplementary Figures and Tables

Fig. S1 Structure of additive CGMs.

Fig. S2 XRD patterns of P-10-80-120 and P-0-80-120 samples crystallizing at 80°C for 3 h and then crystallizing at 120°C for different time.

Fig. S3 XRD patterns of P-10-120 and P-0-120 samples crystallizing at 120°C for different time.

Fig. S4 XRD patterns of P-0-170 and P-10-170 samples crystallizing at 170 °C for different time.

Fig. S5 Dynamic light scattering (DLS) curve of the supernatant of sample P-0-80-120 crystallized at 120 °C for 6 h.

Fig. S6 ²⁹Si MAS NMR spectrum of the supernatant of sample P-0-80-120 crystallized at 120 °C for 6 h.

Fig. S7 ¹³C NMR spectra of samples.

Fig. S8 TEM image, SEM image and particle size distributions of P-10-80-120.

Fig. S9 TEM images of P-10-80-120 sample crystallizing at 80 °C for 3 h and then crystallizing at 120 °C for different time.

Fig. S10 TEM images of P-0-80-120 sample crystallizing at 80 °C for 3 h and then crystallizing at 120 °C for different time.

Fig. S11 XRD patterns of P-S-10-80-120 crystallizing at 80 °C for 3 h and then crystallizing at 120 °C for different time.

Fig. S12 TEM images of P-S-10-80-120 crystallizing at 80 °C for 3 h and then crystallizing at 120 °C for different time.

Fig. S13 FT-IR spectra of P-0-80-120 and P-10-80-120.

Fig. S14 SEM-EDS image and element content analysis of P-10-80-120.

Fig. S15 High-angle annular dark field scanning transmission electron microscopy (HAADF STEM) image and elemental mappings for O, Si and Ti elements of P-10-80-120.

Fig. S16 n(Si/Ti) determined by ICP of P-10-80-120 crystallizing at 80 °C for 3 h and then crystallizing at 120 °C for different time.

Fig. S17 SEM-EDS images and element content analysis of WLPs and small particles of P-10-80-120 crystallizing for 1.5 hours.

Fig. S18 TEM image, HAADF STEM images and elemental mappings for Si and Ti elements of different area in sample P-10-80-120 at 1.5 h.

Fig. S19 UV-vis spectra of P-10-80-120 crystallized at 80 °C for 3 h and then crystallized at 120 °C for different time.

Fig. S20 $n(\text{Si}/\text{Ti})$ determined by ICP of P-0-80-120 crystallizing at 80 °C for 3 h and then crystallizing at 120 °C for different time.

Fig. S21 UV-vis spectra of P-0-80-120 crystallized at 80 °C for 3 h and then crystallized at 120 °C for different time.

Fig. S22 XRD patterns of AM-10-80-120, P800-10-80-120 and P1800-10-80-120.

Fig. S23 XRD patterns of PEI-10-80-120 and PDDA-10-80-120.

Fig. S24 UV-vis spectra of AM-10-80-120, P800-10-80-120, P-10-80-120, P1800-10-80-120, PEI-10-80-120 and PDDA-10-80-120.

Fig. S25 XRD patterns of P-x-80-120 samples.

Fig. S26 FT-IR spectra of P-x-80-120 samples.

Fig. S27 UV-vis spectra of P-x-80-120 samples.

Fig. S28 XPS spectra of Ti 2p in P-x-80-120 samples.

Fig. S29 TEM images, SEM images and particle size distributions of P-x-80-120 samples.

Fig. S30 N_2 adsorption–desorption isotherms and pore size distributions of P-x-80-120 samples.

Fig. S31 SEM image, TEM image, N_2 adsorption–desorption isotherms and UV-vis spectrum of micro-TS-1.

Fig. S32 TEM image and UV-vis spectrum of P-10-80-120-HCl.

Fig. S33 Recycling tests in the oxidation of DBT over the P-10-80-120 sample.

Fig. S34 XRD patterns and UV-vis spectra of the fresh P-10-80-120 sample and the sample after five cycles in the oxidation of DBT.

Fig. S35 Recycling tests in the oxidation of 1-hexene over the P-10-80-120 sample.

Fig. S36 XRD patterns and UV-vis spectra of the fresh P-10-80-120 sample and the sample after four cycles in the epoxidation of 1-hexene.

Table S1 Molar compositions of the initial reaction mixtures and crystallization conditions of TS-1 zeolites.

Table S2 Textural properties of synthesized TS-1 samples.

Table S3 Si/Ti ratio of synthesized samples.

Table S4 Oxidation of 1-hexene over synthesized TS-1 samples.

Experimental section

Reactant agents. Tetraethyl orthosilicate (TEOS, Sinopharm), tetrabutyl orthotitanate (TBOT, Sinopharm, 98%), tetrapropylammonium hydroxide solution (TPAOH; Guangfu Fine Chemical Research Institute, 25 wt%), cationic polyacrylamide (PAM; MW=8000000-15000000, Guangfu Fine Chemical Research Institute), cationic polyacrylamide (PAM, MW=8000000, Adamas), cationic polyacrylamide (PAM, MW=18000000, Adamas), acrylamide (AM, Tianjin Fuchen Chemical Reagent Factory), polydimethyldiallyl ammonium chloride (PDDA, MW=400000-500000, Aladdin, 20 wt%), polyethyleneimine (PEI, MW=10000, Aladdin, 99 %), anatase (Alfa Aesar, 99.9 %), HCl (Beijing Chemical Works, 36 wt%), dibenzothiophene (DBT, Innochem Science & Technology), Tert-butyl hydroperoxide (TBHP, 70 wt% aqueous solution, Alfa Aesar (China) Chemicals), n-octane (Tianjin Fuchen Chemical Reagent Factory), n-hexadecane (Tianjin Fuchen Chemical Reagent Factory), 1-hexene (Aladdin, 99 %), methanol (Tiantai Fine Chemical Research Institute, 99.5 %) and n-dodecane (Aladdin). All the above materials were purchased commercially and used directly without further purification.

Syntheses of PAM- assisted TS-1 zeolites. PAM-assisted TS-1 zeolite was synthesized through a two-step hydrothermal route under static conditions from the starting gels with the molar compositions of SiO_2 : 0.033 TiO_2 : 0.27 TPAOH: 30 H_2O : 0.1 PAM. Typically, the TPAOH solution was mixed with water under stirring. Then, TBOT and TEOS were added to the TPAOH solution to form a clear solution under continuous stirring. After complete hydrolysis of TEOS and TBOT, PAM was added into the above solution. The reaction mixture was further stirred for another 24 hours until the solution becomes uniform. Finally, the resulting solution was transferred into a Teflon-lined stainless-steel autoclave and then crystallized in a pre-heated oven at 80 °C for 3 hours, and then at 120 °C for 3 hours under static conditions. The as-synthesized solid products were centrifuged, washed with distilled water several times, and dried at 80 °C in an oven overnight, then followed by calcination at 550 °C for 6 hours. This sample is named as P-10-80-120. Furthermore, samples with different PAM additions were also synthesized by using the similar synthetic method, which are defined as P-x-80-120, where x represents the molar ratio of PAM to SiO_2 times 10^2 employed in the synthesis.

In order to reveal the effect of the molecular weight of PAM polymer and other polymers on the crystallization of TS-1, TS-1 zeolites with different polymers were synthesized under the same conditions as P-10-80-120. The detailed synthetic conditions for these samples are listed in Table S1.

In order to reveal the role of PAM in the synthesis of TS-1 zeolite, TS-1 zeolites in a two-step crystallization with different times, and a single crystallization at 120 °C and at 170 °C have been prepared. Also, pure silicon silicalite-1 zeolite (named as P-S-10-80-120), and traditional microporous TS-1 (named micro-TS-1) have been synthesized for comparison. The detailed synthetic conditions for these samples are listed in Table S1.

Syntheses of control and acid treated TS-1 zeolites. Control TS-1 zeolite named P-0-80-120 was synthesized with the same molar composition of the P-10-80-120 sample without adding PAM. The control sample was crystallized in a pre-heated oven at 80 °C for 3 hours, and then at 120 °C for 6 hours under static conditions. In addition, to explore the influence of TiO₆ species on catalytic activity of TS-1 zeolite, the sample of P-10-80-120 was washed to eliminate most TiO₆ species. Typically, 1 g P-10-80-120 sample was treated with 100 mL 1M HCl water solution at room temperature for 6 h, and then thoroughly washed with distilled water.

Characterizations

The crystallinity and phase purity of the samples were determined by powder X-ray diffraction (XRD) on Rigaku Ultima IV diffractometer with Cu Ka radiation ($\lambda=1.5418 \text{ \AA}$). Nitrogen adsorption/desorption measurements were carried out on a Micromeritics 2020 analyzer at 77.3 K after degassing the samples at 350 °C under vacuum. Chemical compositions were determined by Inductively Coupled Plasma (ICP) analysis using an iCAP 7000 SERIES. X-ray photoelectron spectroscopy (XPS) was performed with an ESCALAB 250 X-ray photoelectron spectrometer using Al as the excitation source. Scanning electron microscopy (SEM) and transmission electron microscopy (TEM) images were collected using a JSM-6510 (JEOL) electron microscope and a FEI Tecnai F20 electron microscope operating at an acceleration voltage of 200 kV, respectively. Atomic Force Microscope (AFM) images were recorded in the tapping mode from Dimension Fastscan Bio (Bruker) under ambient conditions. X-ray absorption near-edge structure (XANES) spectra at the Ti K-edge were performed using the Sector 20-BM beamline of the

Advanced Photon Source at Argonne National Laboratory (Argonne, IL). The beamline was equipped with a doublecrystal Si(111) monochromator. A 12-element Ge fluorescence detector was used to collect the spectra of the Ti K-edge. The energy was calibrated according to the absorption edge of a pure Ti foil as a reference. Data processing and EXAFS fitting were performed using the Athena, Artemis and Igor software. Elemental analysis of samples was investigated by the X-ray energy dispersive spectra (EDS, Quantax EDS spectroscopy, Bruker). Ti species were investigated by UV-vis diffuse reflectance spectroscopy (UV-Vis) over a range of 200 to 600 nm using a SHIMADZU U-4100. The baseline correction was carried out with powder BaSO₄. Fourier transform infrared (FT-IR) spectra were recorded on a BRUKER vertex 80v, samples were pelleted with KBr powder before testing. Thermal gravimetric (TG) analyses were performed using a TA TGA Q500 at temperatures ranging from room temperature to 800 °C at a heating rate of 10 °C min⁻¹. ²⁹Si solid state magic angle rotation nuclear magnetic resonance (SS MAS NMR) and ¹H→¹³C CP MAS NMR were collected on Bruker Avance NEO 600WB system. Kaolin and Adamantane (Adam) was used as the standard sample of ²⁹Si and ¹³C, respectively. And the calibration of ²⁹Si and ¹³C were -91.4 ppm and 38.48 ppm, respectively. For the liquid NMR measurement of the supernatant of sample, the supernatant was mixed with deuterium oxide (D₂O) for field locking, and then placed in polytetrafluoroethylene (PTFE) sample tubes for NMR measurement. Tetramethylsilane was used as standard sample, the calibration of ²⁹Si was 0 ppm. The dynamic light scattering test was carried out on Malvern Zetasizer Nano-ZS.

Catalytic tests

Oxidative desulfurization of dibenzothiophene (DBT). A certain amount of DBT was dissolved in n-octane to prepare the model fuel with the concentration of sulfur is about 500 ppm. The ODS reactivity was tested in a 25 mL two-neck glass flask equipped with a reflux condenser. In a typical run, the reaction was carried out with 10 mL model fuel, 0.10 g of zeolite catalyst, 0.028 g of n-octadecane and 0.028 g of TBHP at 353 K for 120 min. Afterwards, GC-MS (Thermo Fisher Trace ISQ, equipped with a TG-5MS column, 60 m 320 μm 25 μm) was utilized to analyse the reactant and products.

Epoxidation of 1-hexene. Epoxidation of 1-hexene with H₂O₂ as oxidant was carried out in a 25 mL round-bottom flask equipped with a reflux condenser. In a typical operation, 0.05 g of catalyst, 10 mL of

methanol, 10 mmol of 1-hexene and 3.3 mmol H₂O₂ (30 wt%) were added into a double-necked round bottom flask in sequence, and the reaction was carried out under continual magnetic stirring at 333 K for 120 min. Upon completion of the reaction, the liquid product was centrifuged and analyzed by GC-MS (Thermo Fisher Trace ISQ, equipped with a TG-5MS column, 60 m 320 μm 25 μm) and n-dodecane as internal standard. The conversion of 1-hexene and the selectivity of corresponding epoxy compounds were calculated. The conversion and efficiency of H₂O₂ were determined by iodometric method.

Supplementary Figures and Tables

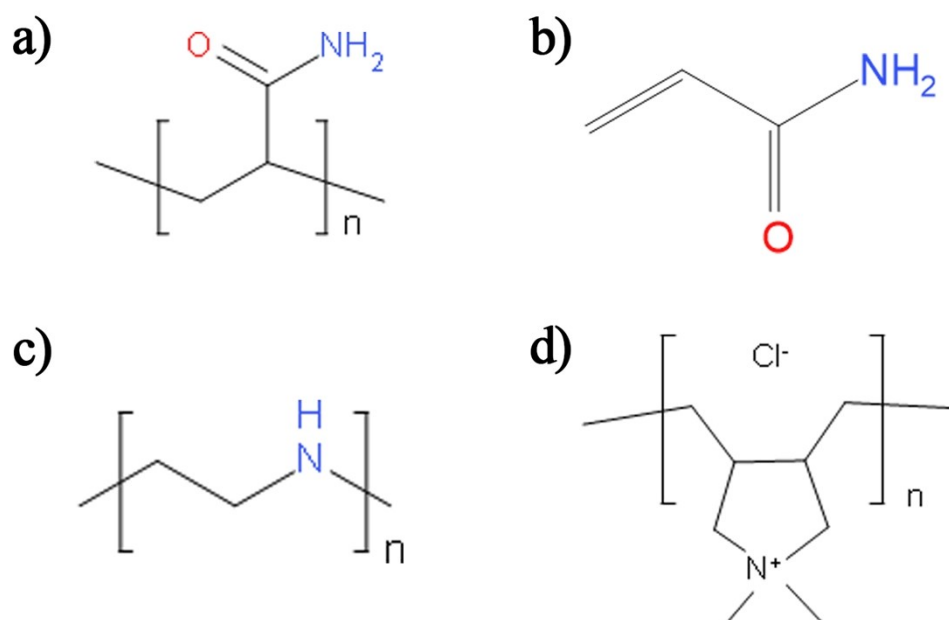


Fig. S1 Structures of a) polyacrylamide (PAM), b) acrylamide (AM), c) polyethyleneimine (PEI) and d) polydimethyldiallyl ammonium chloride (PDDA).

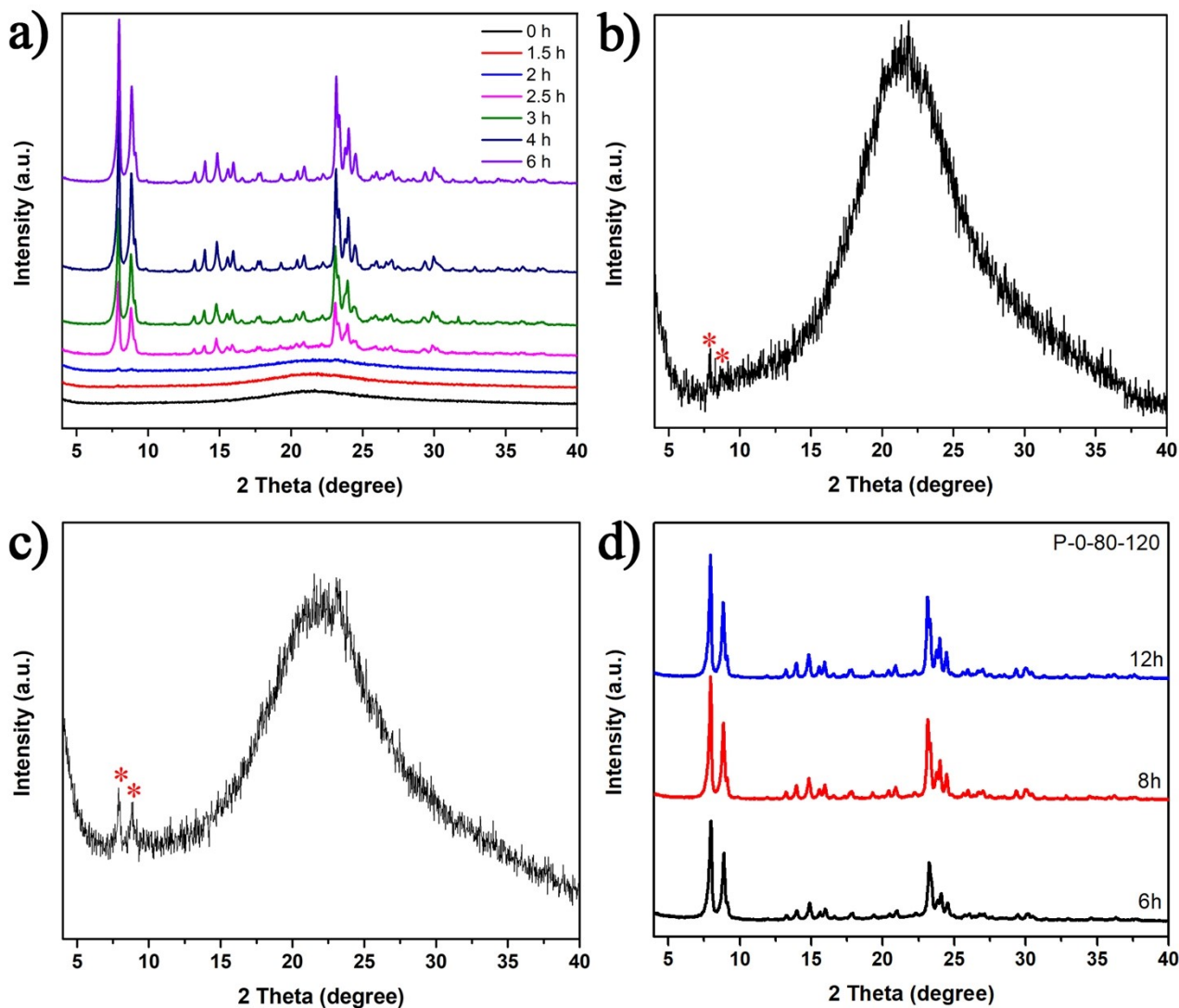


Fig. S2 XRD patterns of P-10-80-120 samples crystallizing at 80 °C for 3 h and then crystallizing at 120 °C for a) different time, b) 1.5 h and c) 2 h, and d) P-0-80-120 samples crystallizing at 80 °C for 3 h and then crystallizing at 120 °C for different time.

Note: The induction period of nucleation was estimated from the powder XRD pattern of the extracted solid according to the initial characteristic diffraction peak. Since no crystal appeared in P-0-80-120 before 6 h (120 °C), the induction time was determined to be 9 h (80 °C for 3 h and 120 °C for 6 h), while P-10-80-120 was 4.5 h (80 °C for 3 h and 120 °C for 1.5 h).

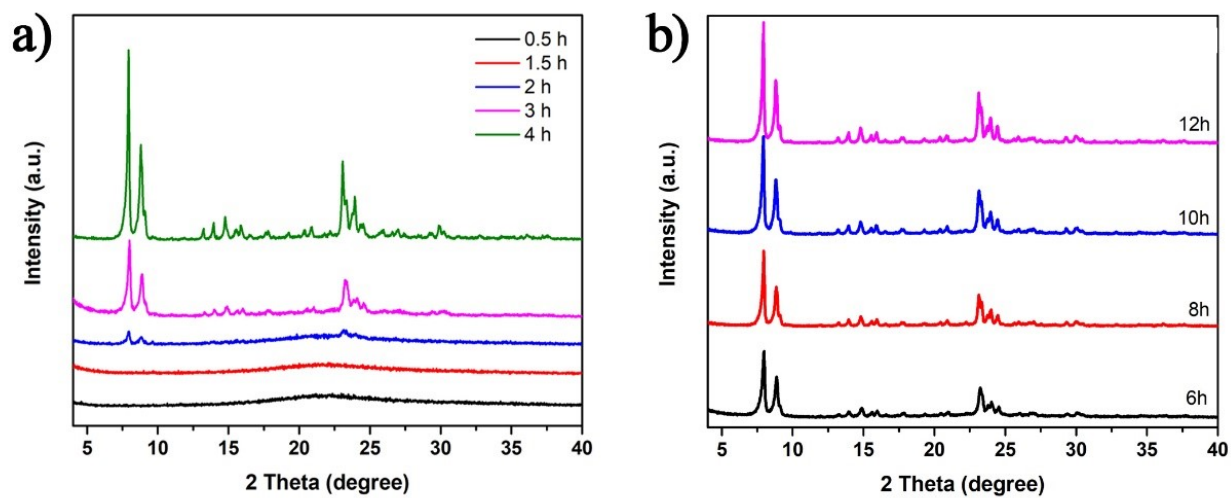


Fig. S3 XRD patterns of a) P-10-120 samples and b) P-0-120 samples crystallizing at 120 °C for different time.

Note: Since no crystal appeared in P-0-120 before 6 h, the induction time was determined to be 6 h, while P-10-80-120 was 2 h.

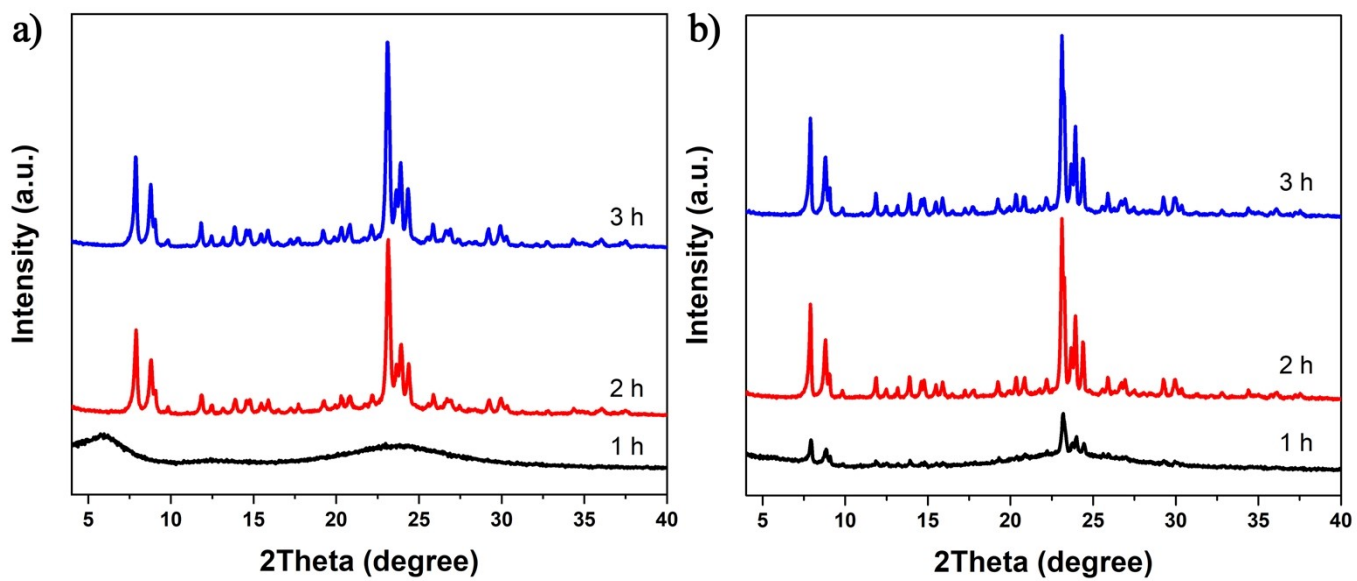


Fig. S4 XRD patterns of a) P-0-170 and b) P-10-170 crystallizing at 170 °C for different time.

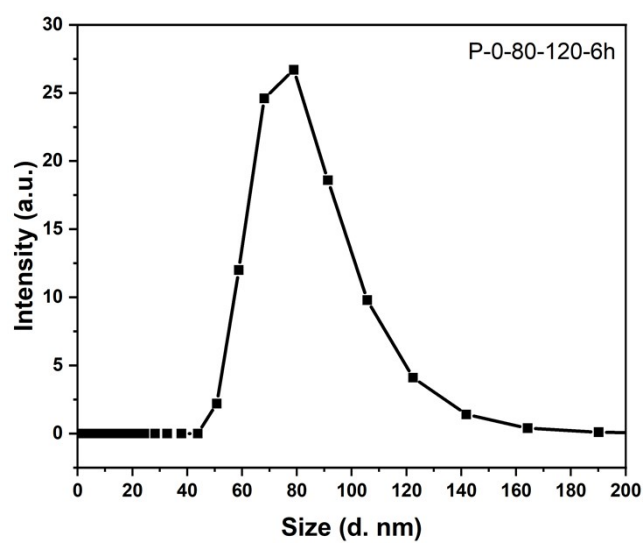


Fig. S5 Dynamic light scattering (DLS) curve of the supernatant of sample P-0-80-120 crystallized at 120 °C for 6 h.

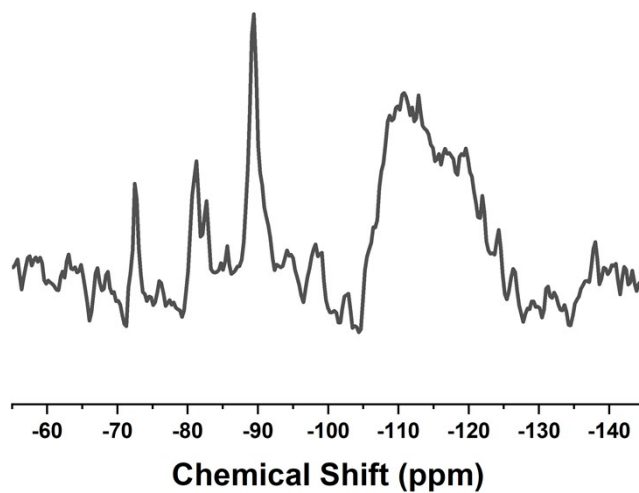


Fig. S6 ^{29}Si MAS NMR spectrum of the supernatant of sample P-0-80-120 crystallized at 120 °C for 6 h.

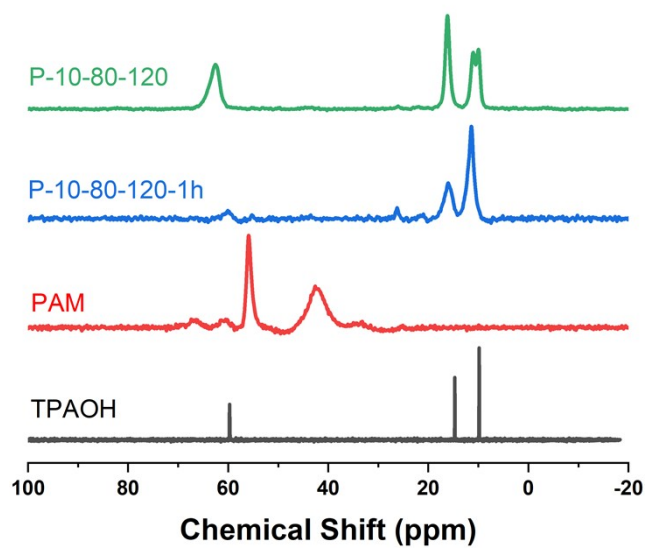


Fig. S7 ¹³C NMR spectra of samples.

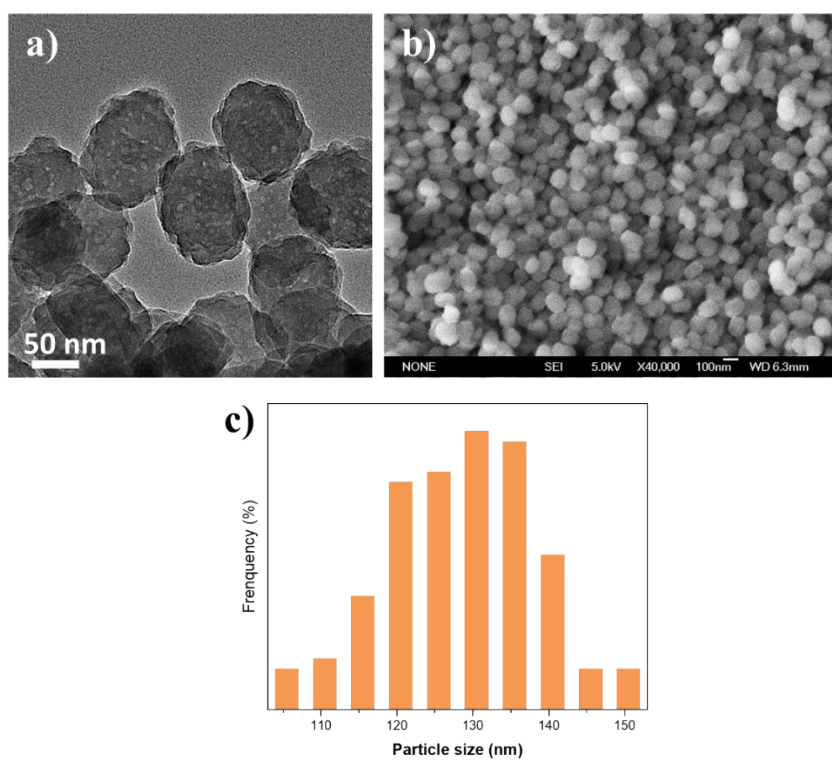


Fig. S8 a) TEM image, b) SEM image, and c) particle size distributions of P-10-80-120.

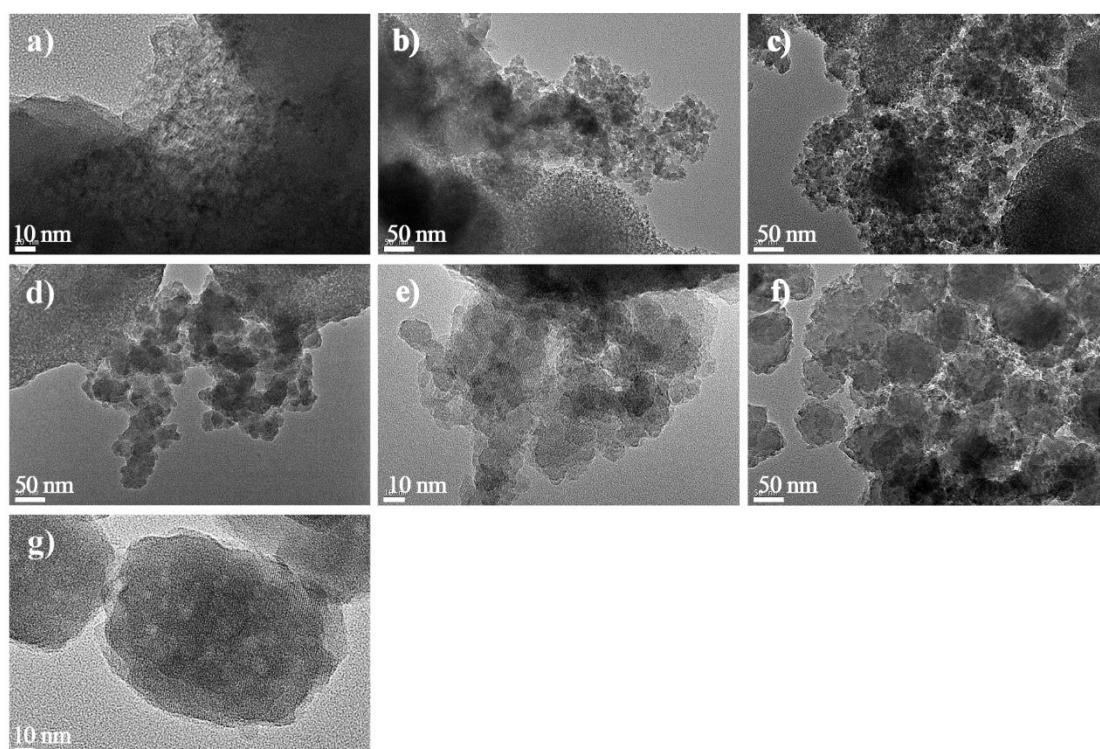


Fig. S9 TEM images of P-10-80-120 sample crystallizing at 80 °C for 3 h and then crystallizing at 120 °C for a) 0 h, b) 0.5 h, c) 1.0 h, d) 1.5 h, e) 2.0 h, f) 2.5 h, g) and 3.0 h.

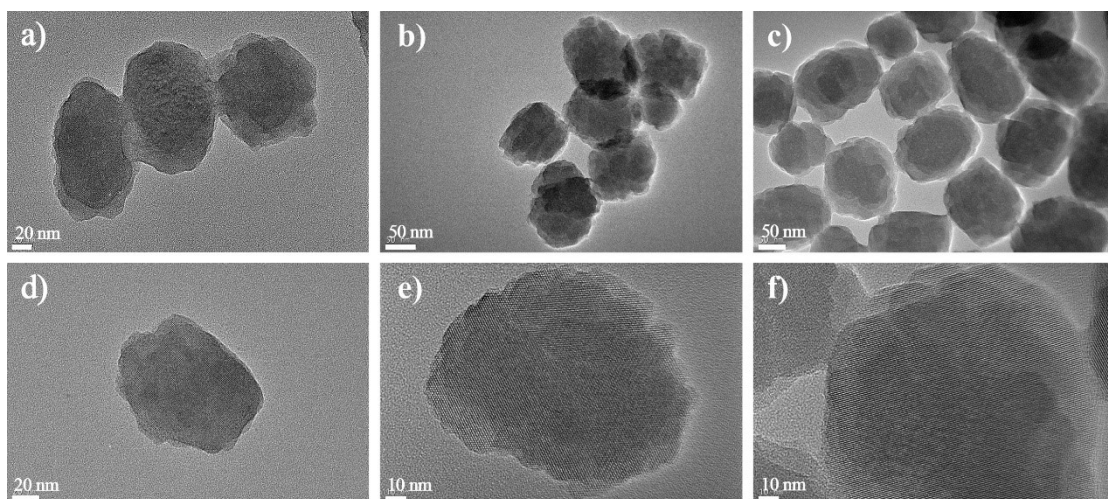


Fig. S10 TEM images of P-0-80-120 sample crystallizing at 80 °C for 3 h and then crystallizing at 120 °C for a) and d) 6 h, b) and e) 8 h, c) and f) 12 h.

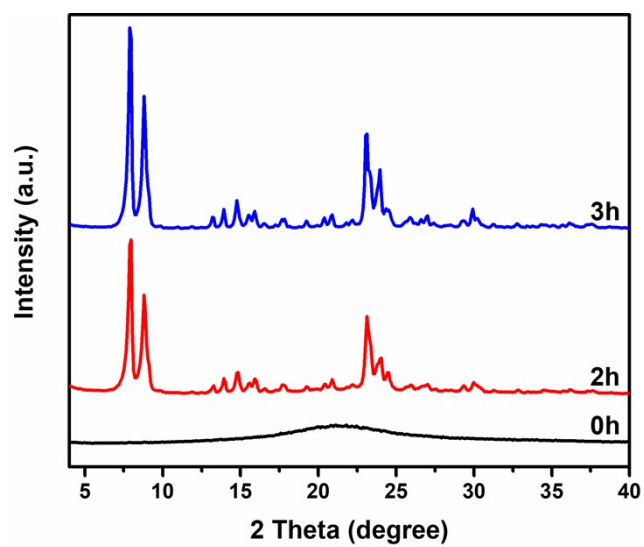


Fig. S11 XRD patterns of P-S-10-80-120 crystallizing at 80 °C for 3 h and then crystallizing at 120 °C for different time.

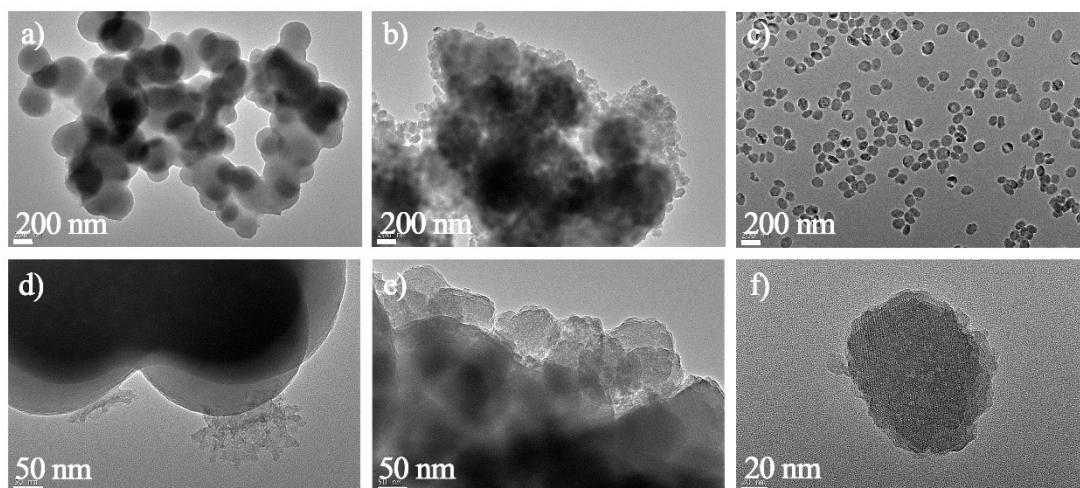


Fig. S12 TEM images of P-S-10-80-120 crystallizing at 80 °C for 3 h and then crystallizing at 120 °C for another a) and d) 0 h, b) and e) 2 h, c) and f) 3 h.

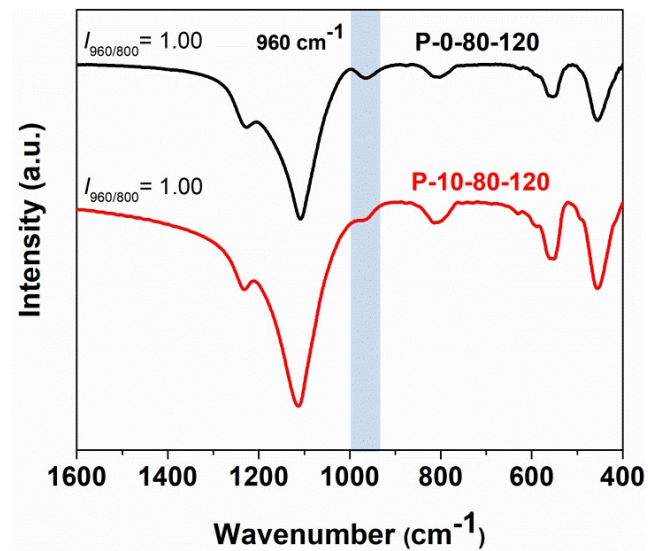
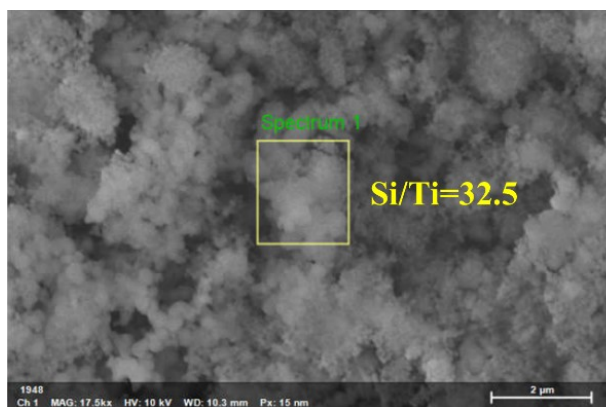


Fig. S13 FT-IR spectra of P-0-80-120 and P-10-80-120.



Spectrum 1

Element	Mass [%]	Mass Norm. [%]	Atom [%]	abs. error [%] (3 sigma)
O	44.29	45.71	56.19	16.66
Si	41.91	43.25	30.28	5.25
C	6.31	6.51	10.66	3.97
Na	2.20	2.27	1.94	0.52
Ti	2.20	2.27	0.93	0.48
	96.90	100.00	100.00	

Fig. S14 SEM-EDS image and element content analysis of P-10-80-120.

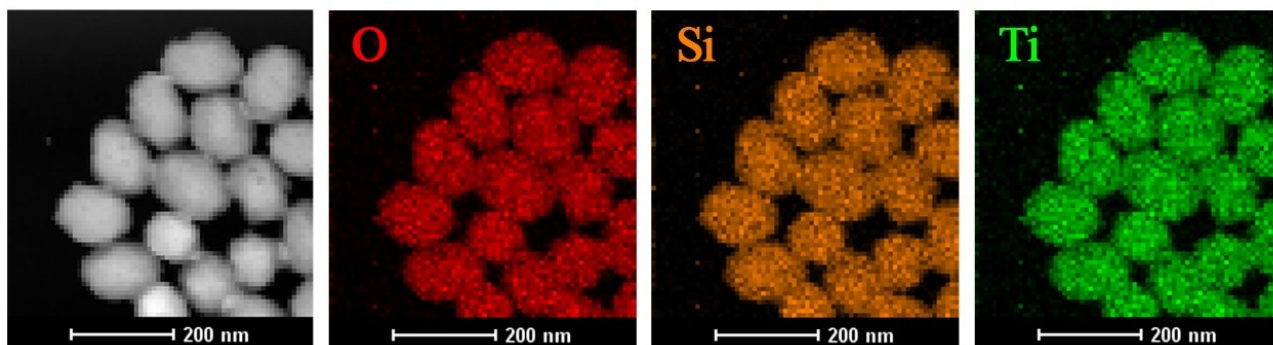


Fig. S15 High-angle annular dark field scanning transmission electron microscopy (HAADF STEM) image and elemental mappings for O, Si and Ti elements of P-10-80-120.

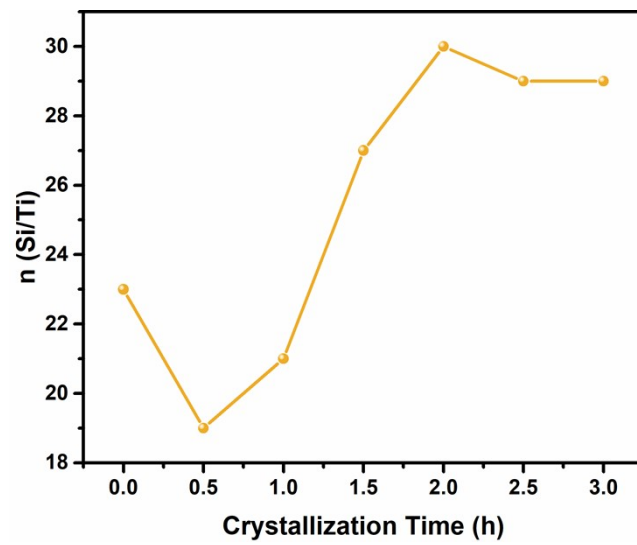


Fig. S16 $n(\text{Si}/\text{Ti})$ determined by ICP of P-10-80-120 crystallizing at 80 °C for 3 h and then crystallizing at 120 °C for different time.

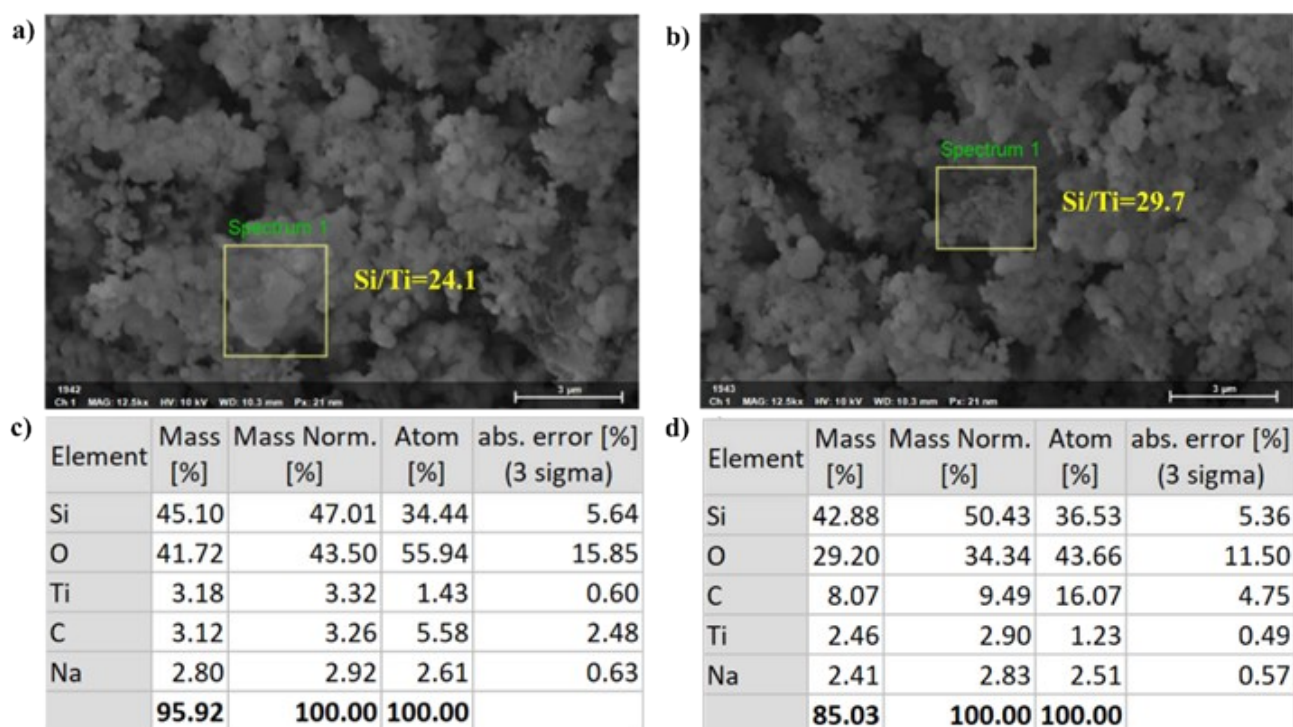


Fig. S17 SEM-EDS images of a) WLPs and b) small particles of P-10-80-120 crystallizing for 1.5 hours and element content analysis of c) WLPs and d) small particles of P-10-80-120 crystallizing for 1.5 hours.

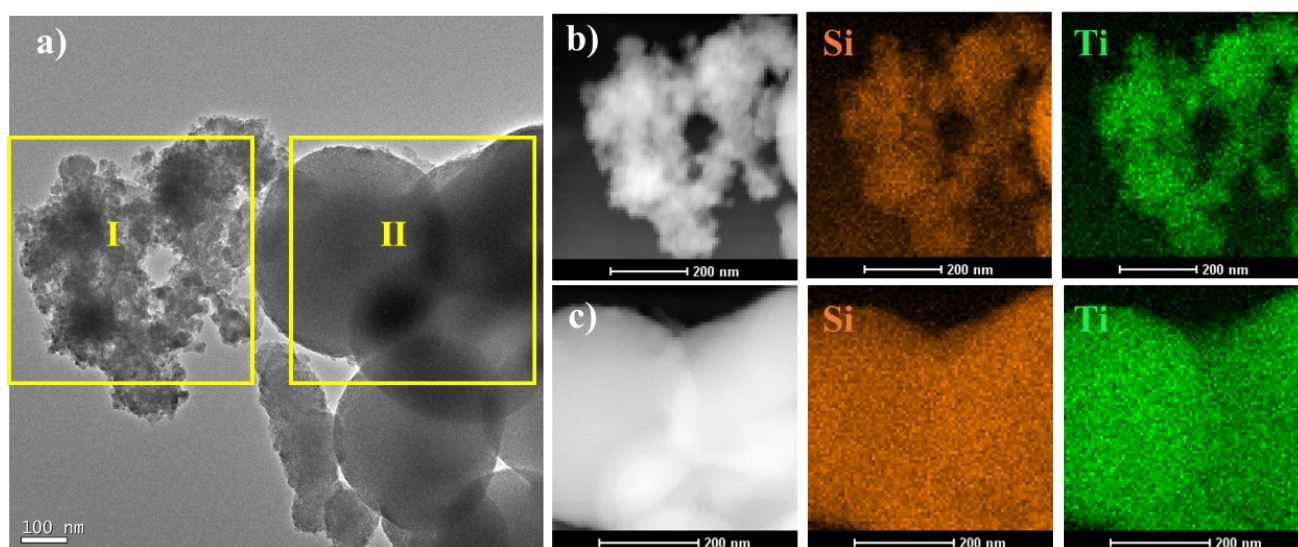


Fig. S18 a) TEM image, HAADF STEM images and elemental mappings for Si and Ti elements of b) area I and c) area II in sample P-10-80-120 at 1.5 h.

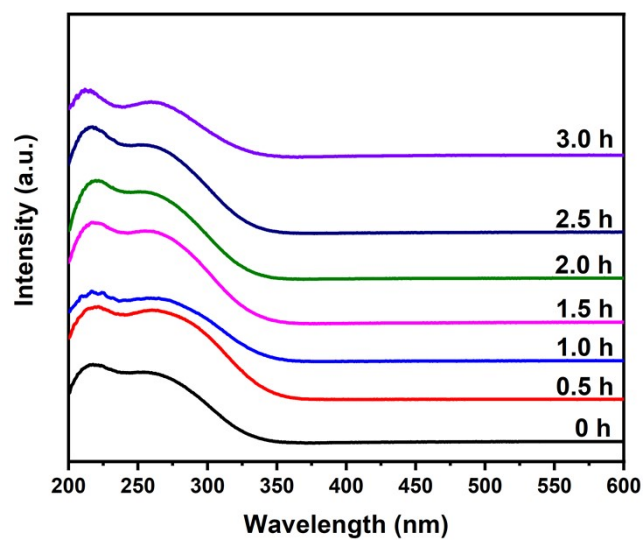


Fig. S19 UV-vis spectra of P-10-80-120 crystallized at 80 °C for 3 h and then crystallized at 120 °C for different time (the data of P-10-80-120 in Fig. 4a is also placed here for comparison).

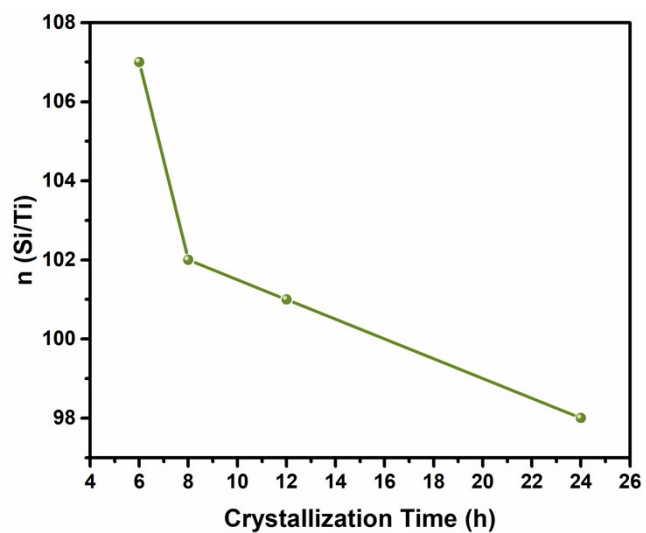


Fig. S20 $n(\text{Si/Ti})$ determined by ICP of P-0-80-120 crystallizing at 80 °C for 3 h and then crystallizing at 120 °C for different time.

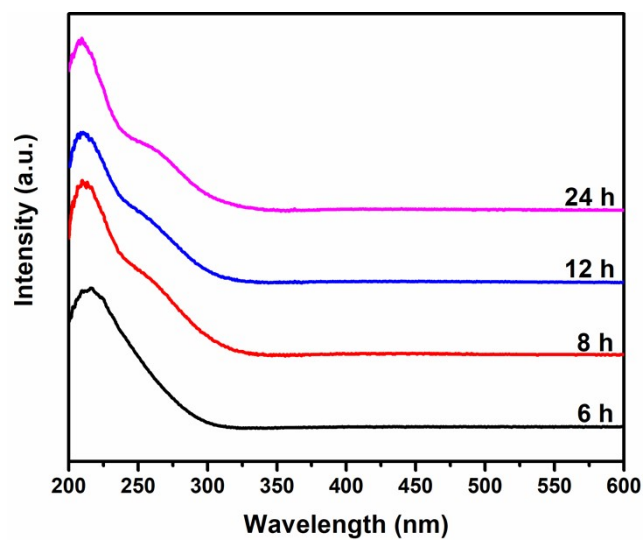


Fig. S21 UV-vis spectra of P-0-80-120 crystallized at 80 °C for 3 h and then crystallized at 120 °C for different time (the data of P-0-80-120 in Fig. 4a is also placed here for comparison).

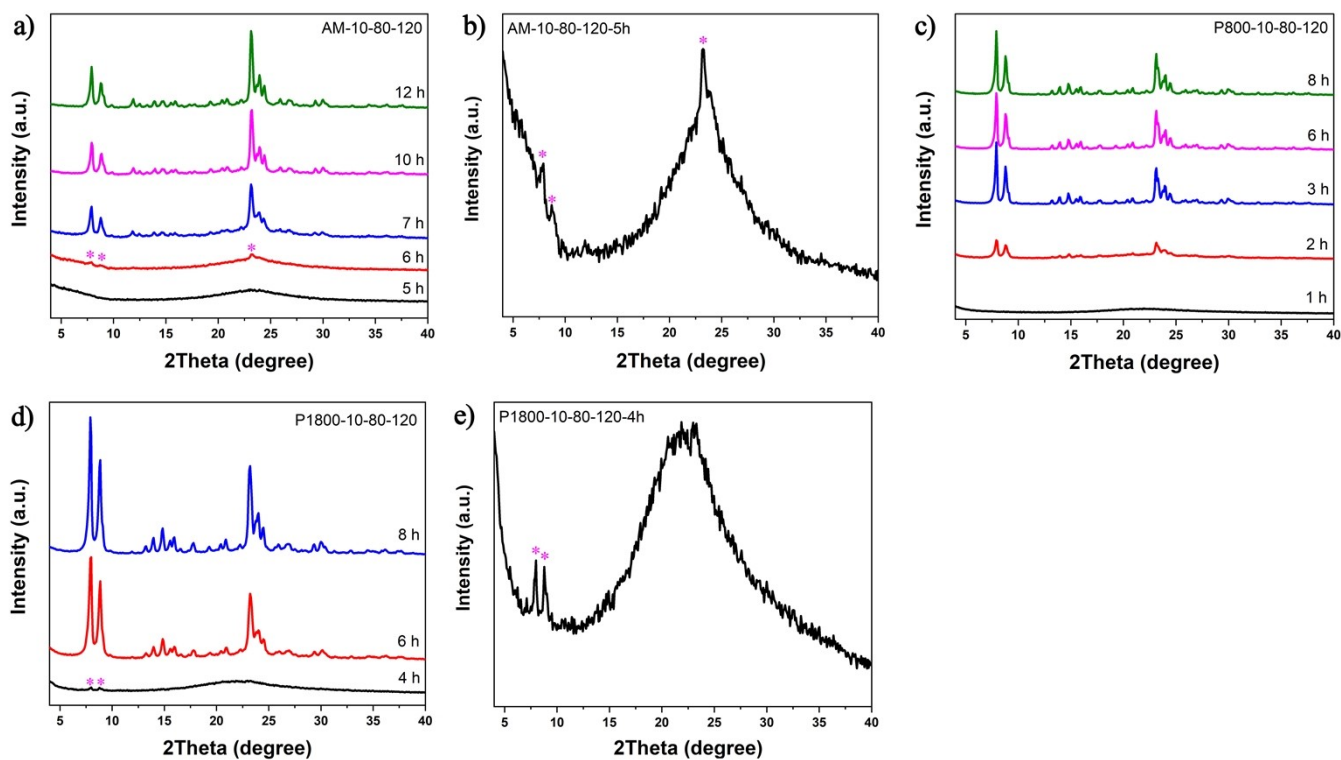


Fig. S22 XRD patterns of a) AM-10-80-120, c) P800-10-80-120, and d) P1800-10-80-120 crystallizing at 80 °C for 3 h and then crystallizing at 120 °C for different time, for b) is 5 h and for e) is 4 h.

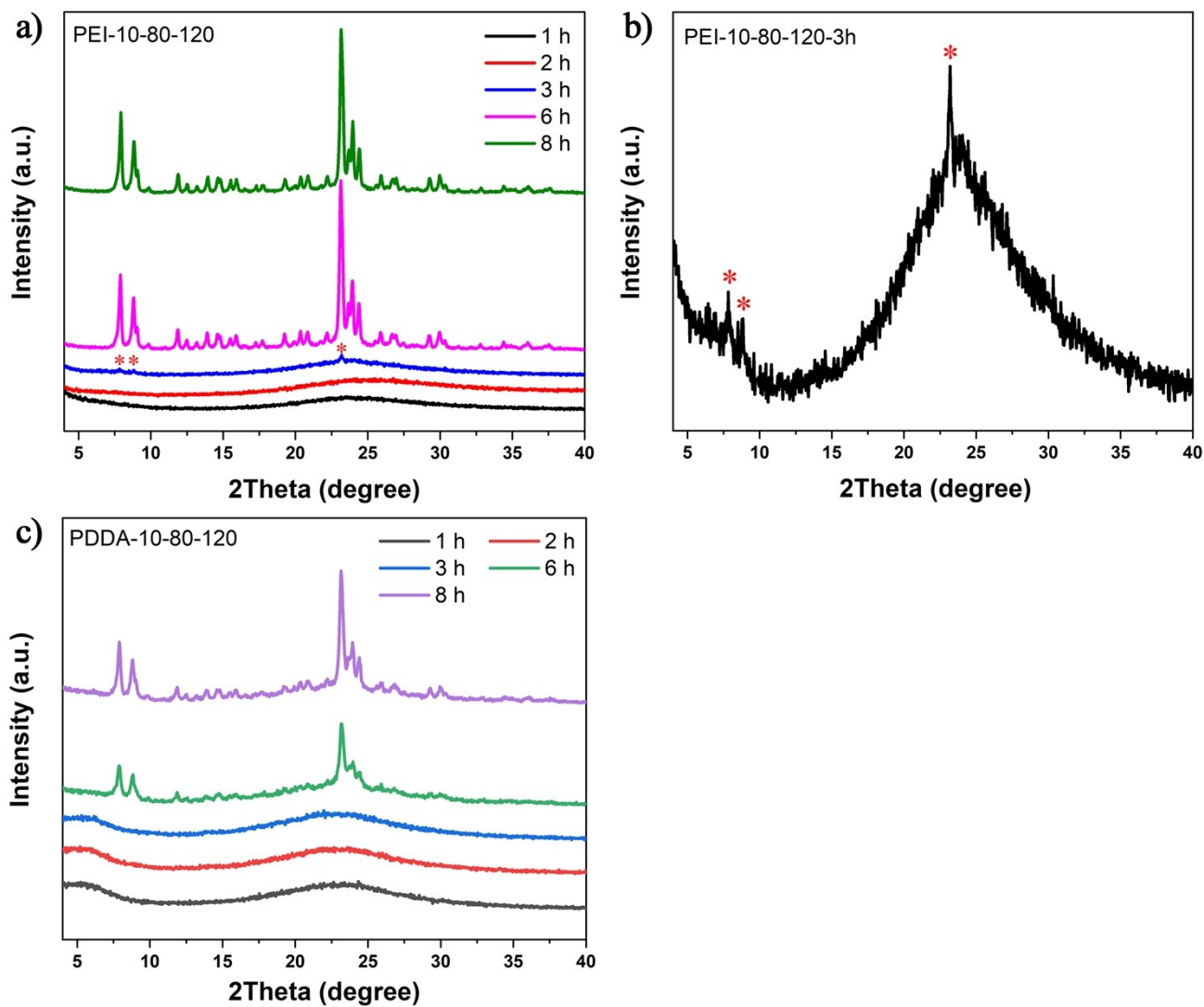


Fig. S23 XRD patterns of a) PEI-10-80-120 and c) PDDA-10-80-120 crystallizing at 80 °C for 3 h and then crystallizing at 120 °C for different time, and for b) is 3 h.

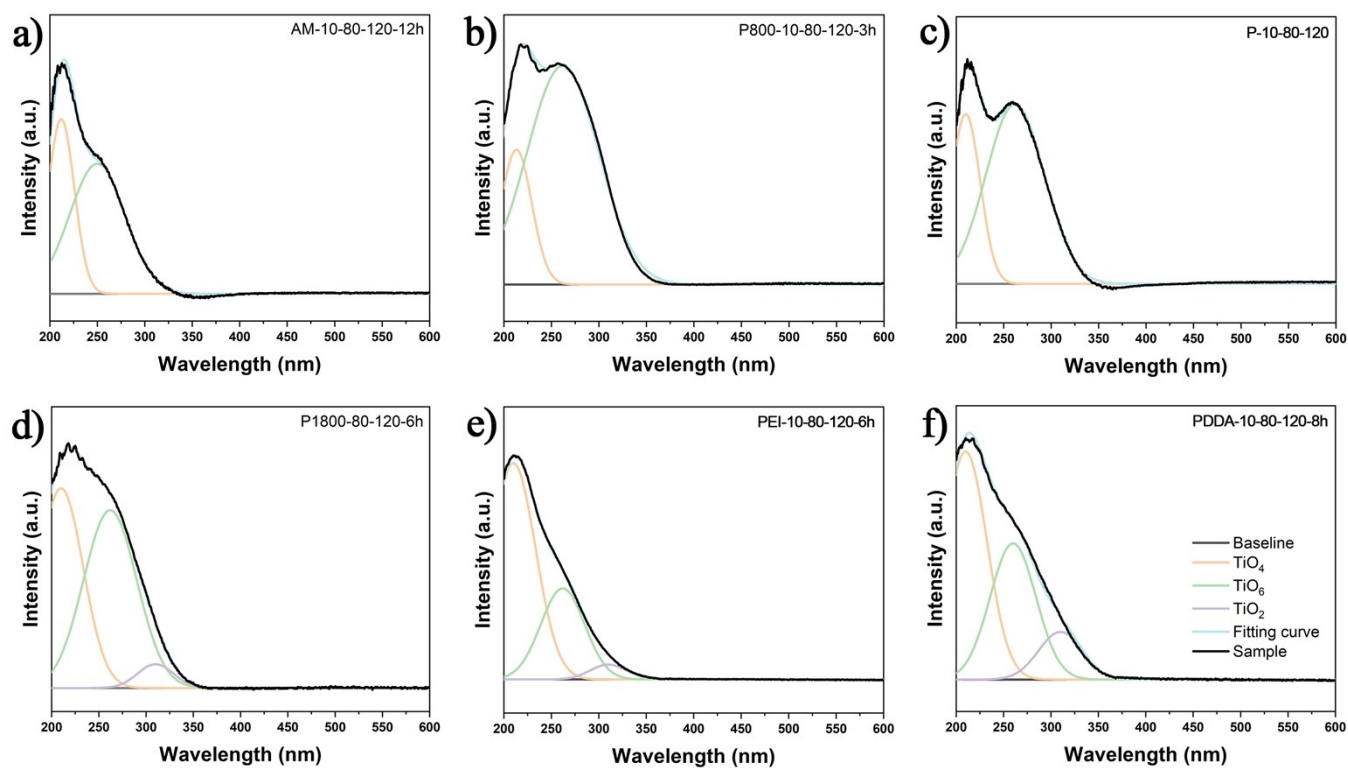


Fig. S24 UV-vis spectra of a) AM-10-80-120, b) P800-10-80-120, c) P-10-80-120, d) P1800-10-80-120, e) PEI-10-80-120 and f) PDDA-10-80-120 (the data of P-10-80-120 in Fig. 4a is also placed here for comparison).

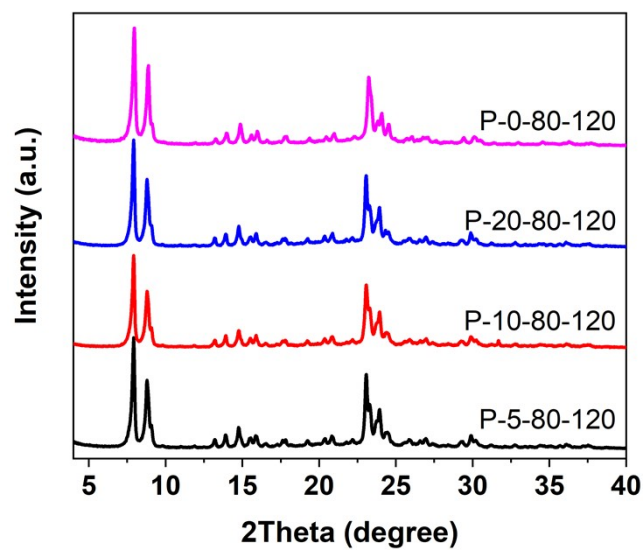


Fig. S25 XRD patterns of P-x-80-120 samples (the data of P-0-80-120 and P-10-80-120 in Fig. S1 is also placed here for comparison).

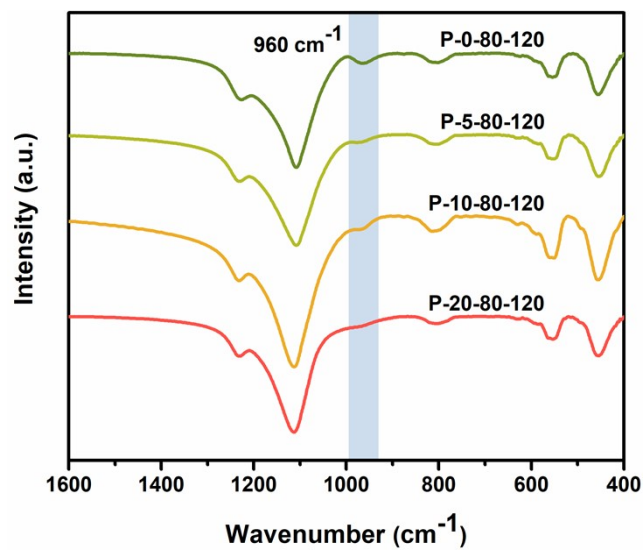


Fig. S26 FT-IR spectra of P-x-80-120 samples (the data of P-0-80-120 and P-10-80-120 in Fig. S10 is also placed here for comparison).

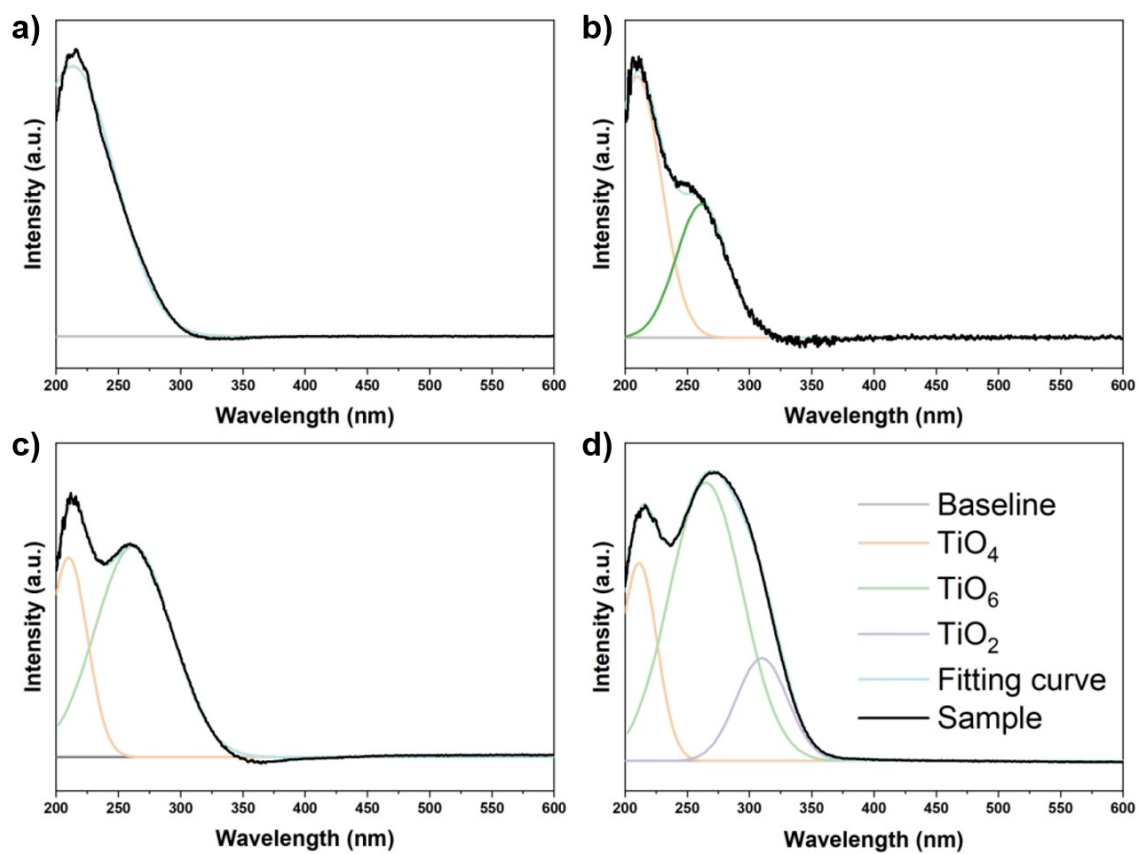


Fig. S27 UV-vis spectra of a) P-0-80-120, b) P-5-80-120, c) P-10-80-120 and d) P-20-80-120 samples (the data of P-0-80-120 and P-10-80-120 in Figure. 4a is also placed here for comparison).

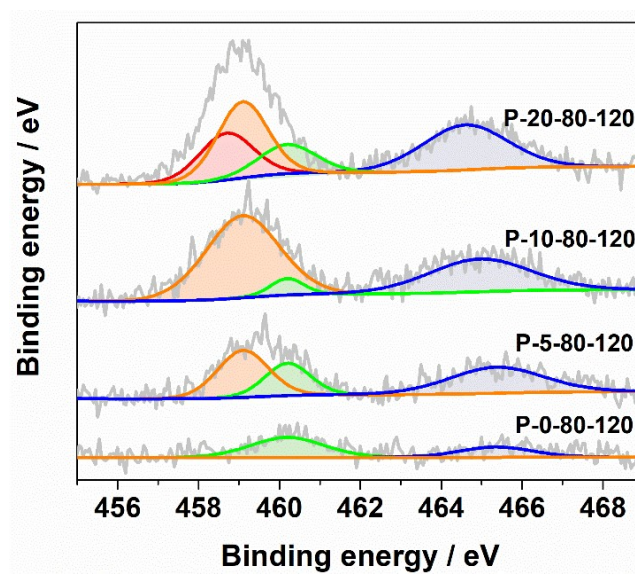


Fig. S28 XPS spectra of Ti 2p in P-x-80-120 samples (the data of P-0-80-120 and P-10-80-120 in Fig. 4b is also placed here for comparison).

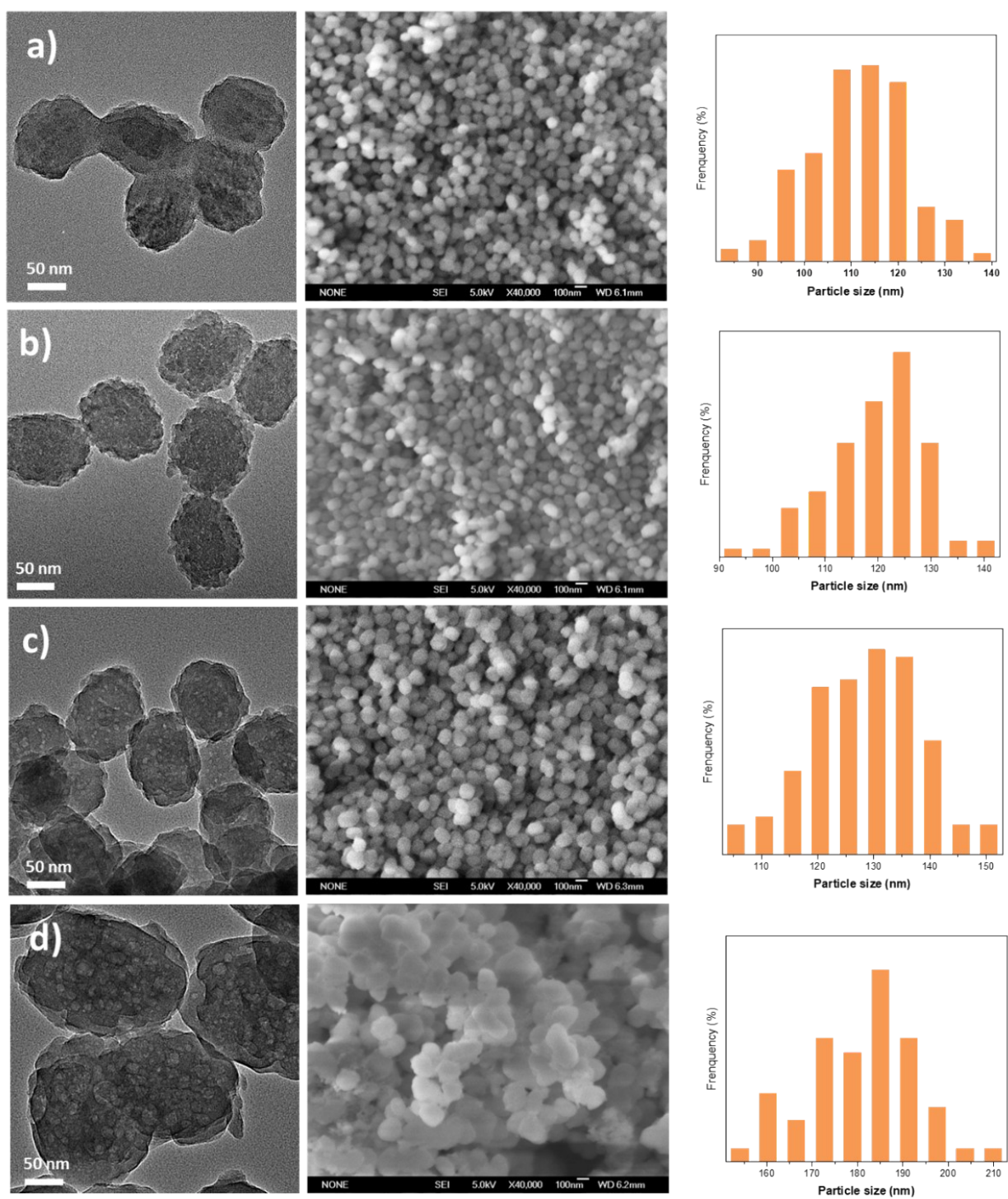


Fig. S29 TEM images, SEM images and particle size distributions of a) P-0-80-120, b) P-5-80-120, c) P-10-80-120 and d) P-20-80-120 (the data of P-10-80-120 in Fig. S3 is also placed here for comparison).

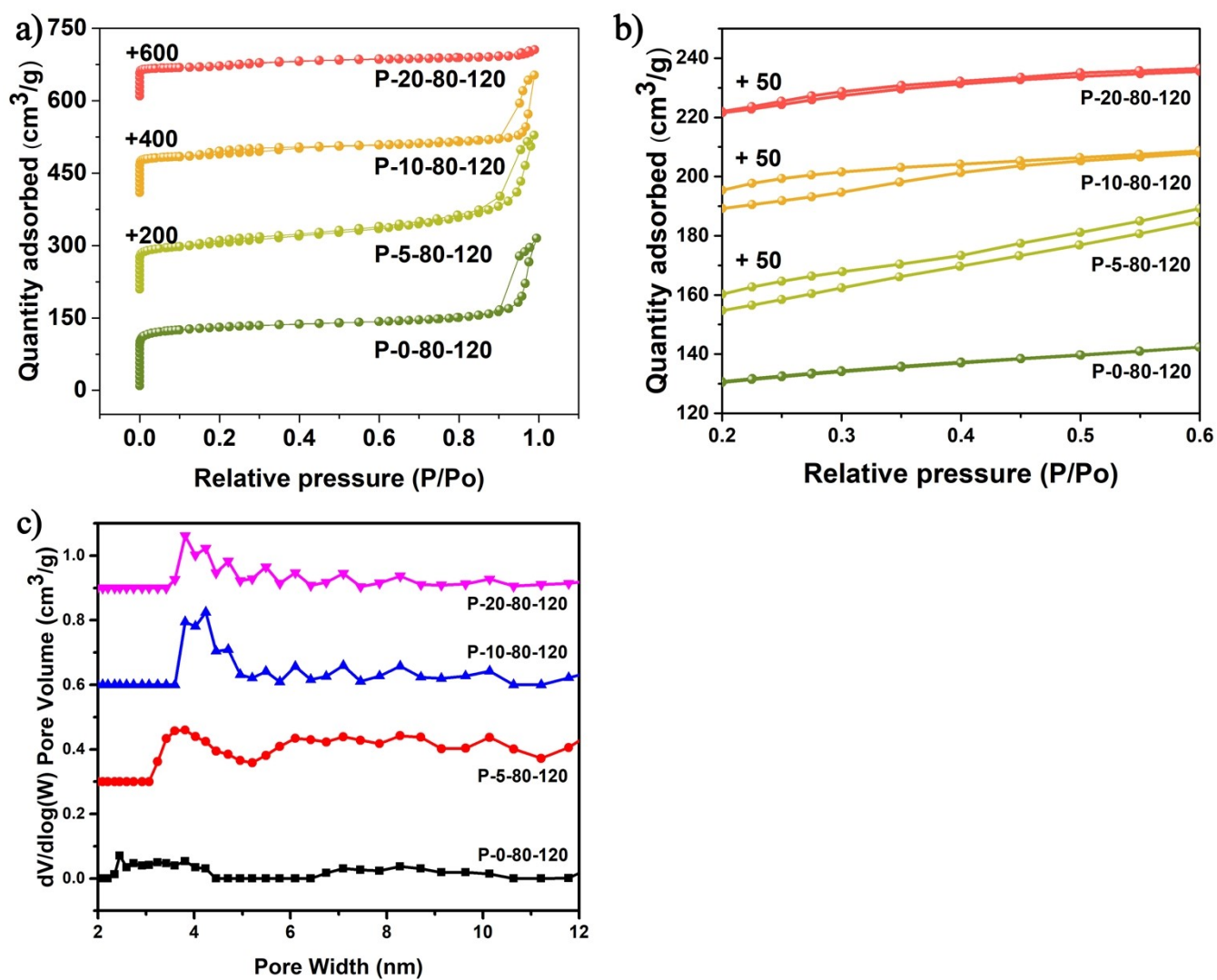


Fig. S30 N_2 adsorption–desorption isotherms in the regions of a) 0.0-1.0 P/P_0 , b) 0.2-0.6 P/P_0 of P-x-80-120 samples and c) pore size distributions of synthesized samples.

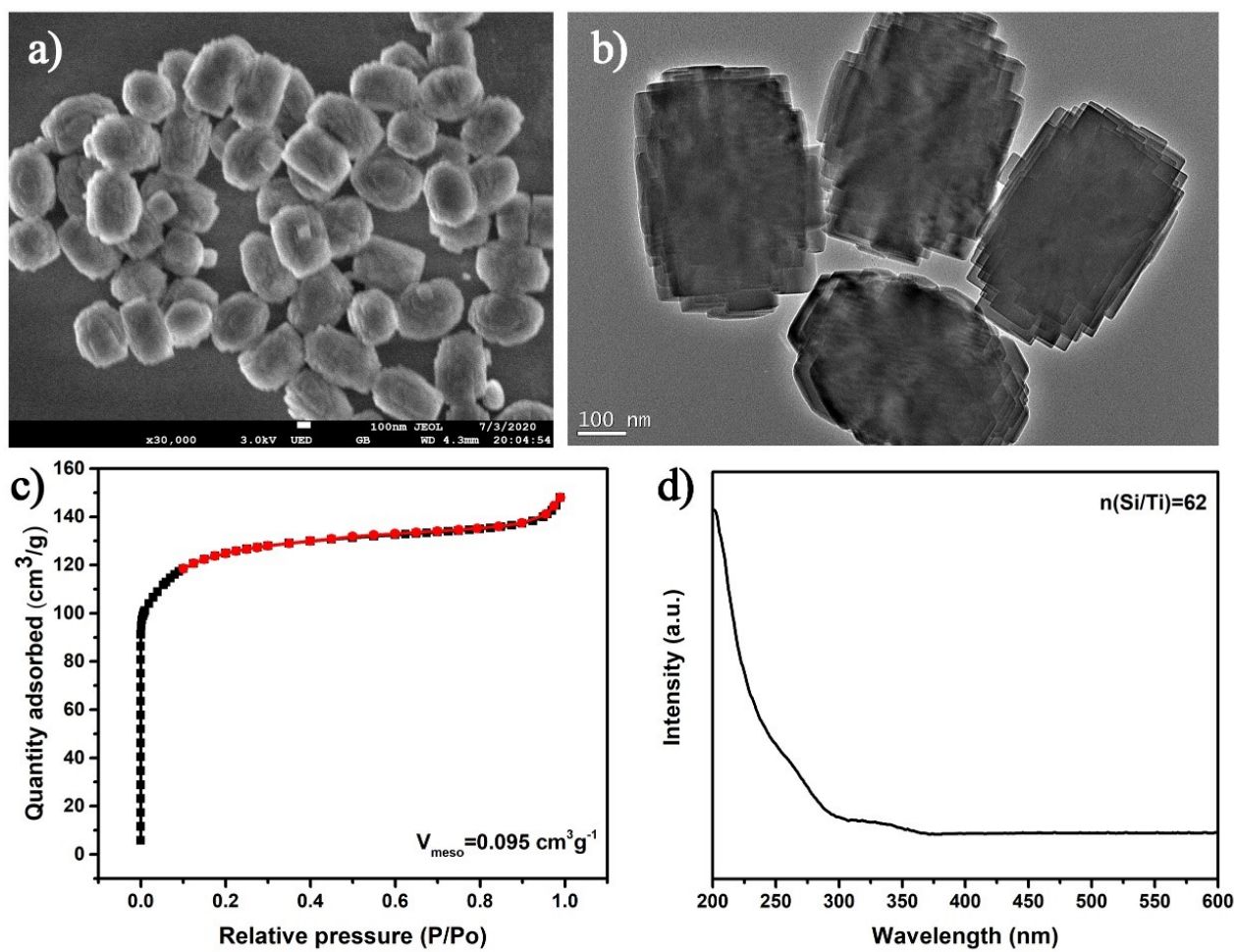


Fig. S31 a) SEM image, b) TEM image, c) N₂ adsorption–desorption isotherms and d) UV-vis spectrum of micro-TS-1 ($n(\text{Si/Ti})$ was determined by ICP).

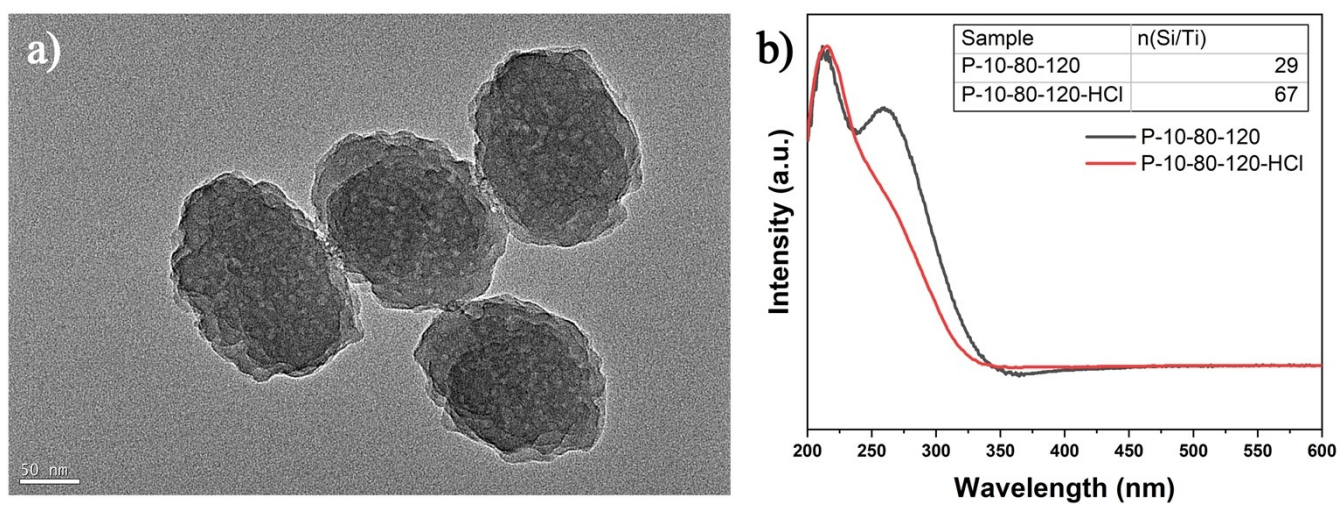


Fig. S32 a) TEM image of P-10-80-120-HCl and b) UV-vis spectra of P-10-80-120 and P-10-80-120-HCl (the inserted table is n(Si/Ti) of samples determined by ICP).

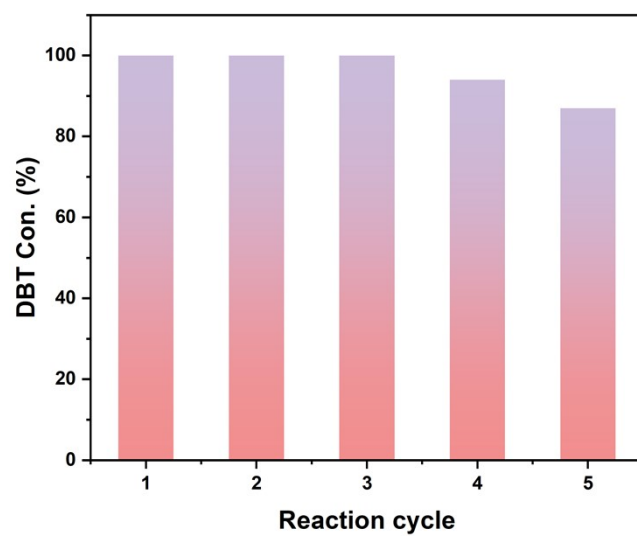


Fig. S33 Recycling tests in the oxidation of DBT over the P-10-80-120 sample.

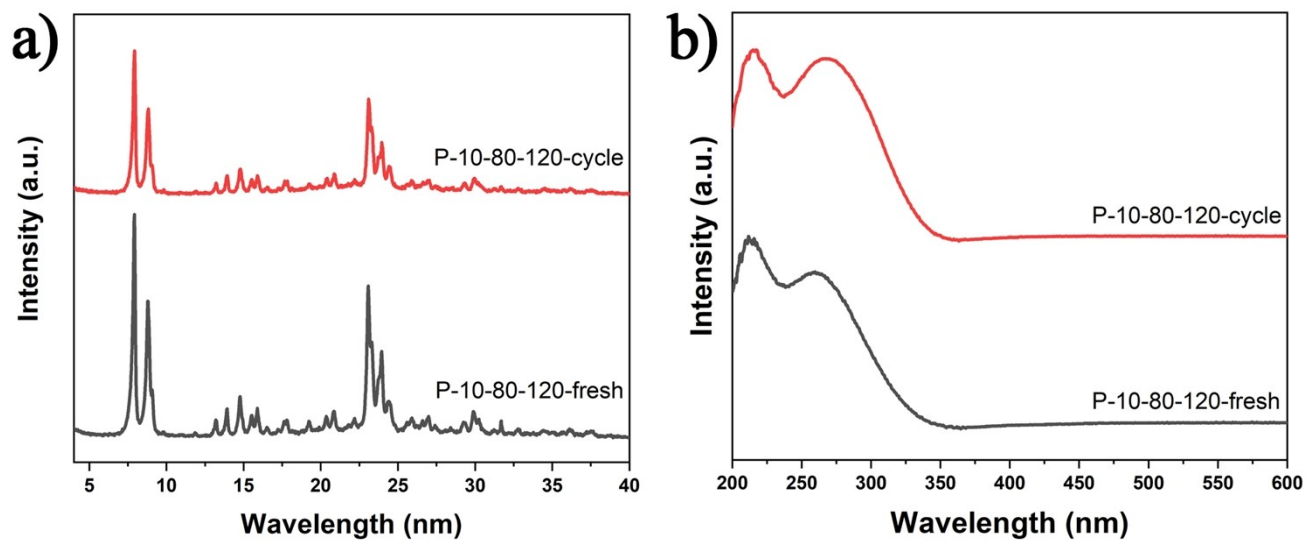


Fig. S34 a) XRD patterns and b) UV-vis spectra of the fresh P-10-80-120 sample and the sample after five cycles in the oxidation of DBT.

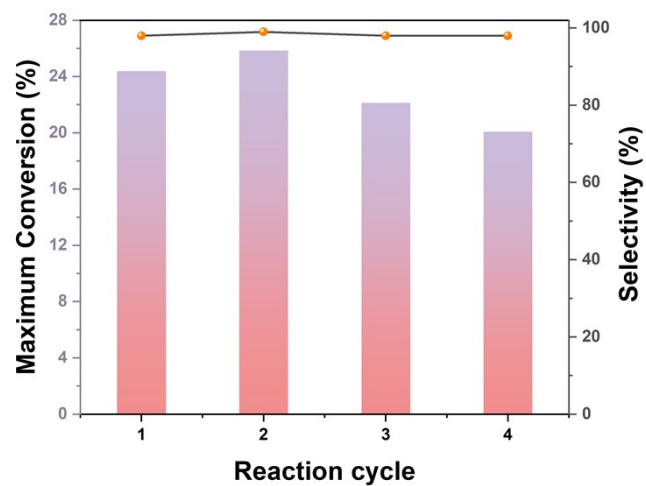


Fig. S35 Recycling tests in the oxidation of 1-hexene over the P-10-80-120 sample.

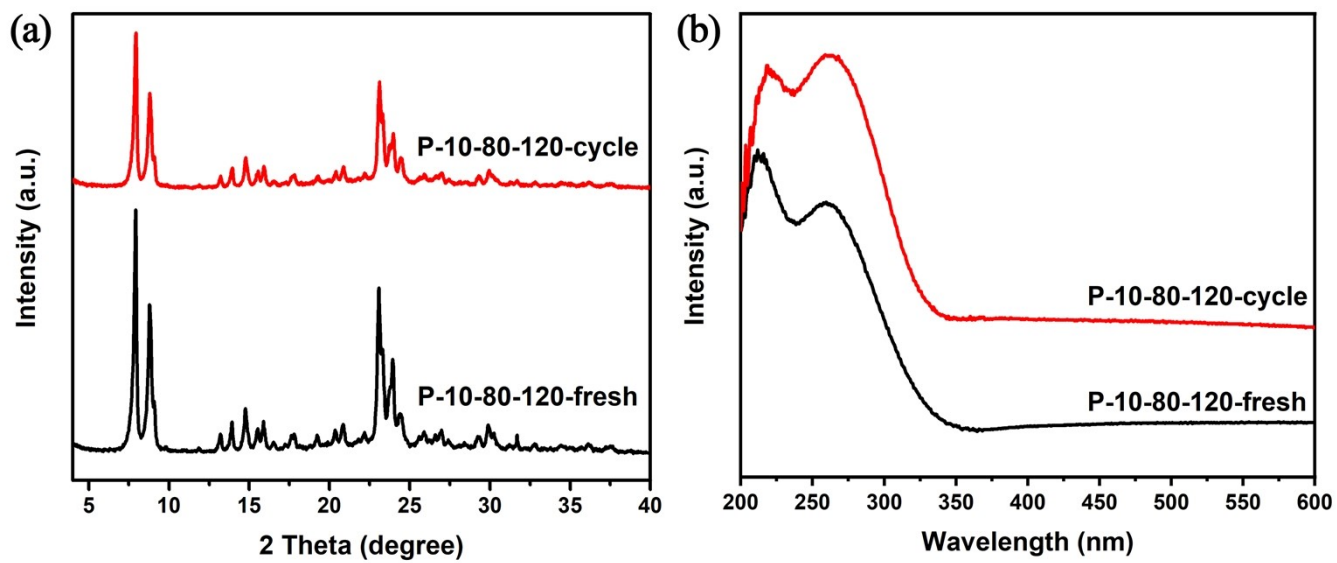


Fig. S36 a) XRD patterns and b) UV-vis spectra of the fresh P-10-80-120 sample and the sample after four cycles in the epoxidation of 1-hexene.

Table S1. Molar compositions of the initial reaction mixtures and crystallization conditions of TS-1 zeolites.^a

	SiO ₂	TiO ₂	Name of CGM	CGM	Temperature (time)
P-0-80-120	1	0.033			80 °C (3 h) + 120 °C (6 h)
P-5-80-120	1	0.033	PAM ^b	0.05	80 °C (3 h) + 120 °C (3 h)
P-10-80-120	1	0.033	PAM	0.10	80 °C (3 h) + 120 °C (3 h)
P-20-80-120	1	0.033	PAM	0.20	80 °C (3 h) + 120 °C (3 h)
P-0-120	1	0.033			120 °C (6 h)
P-10-120	1	0.033	PAM	0.10	120 °C (3 h)
P-0-170	1	0.033			170 °C (3 h)
P-10-170	1	0.033	PAM	0.10	170 °C (3 h)
AM-10-80-120	1	0.033	AM	0.10	80 °C (3 h) + 120 °C (12 h)
P800-10-80-120	1	0.033	PAM (MW=8000000)	0.10	80 °C (3 h) + 120 °C (3 h)
P1800-10-80-120	1	0.033	PAM (MW=18000000)	0.10	80 °C (3 h) + 120 °C (8 h)
PEI-10-80-120	1	0.033	PEI	0.10	80 °C (3 h) + 120 °C (6 h)
PDDA-10-80-120	1	0.033	PDDA	0.10	80 °C (3 h) + 120 °C (8 h)
P-S-10-80-120	1	0	PAM	0.10	80 °C (3h) + 120 °C (3h)
micro-TS-1	1	0.014			170 °C (36 h)

^aThe ratios of TPAOH/SiO₂ and H₂O/SiO₂ are 0.27 and 30, respectively. The ratio of H₂O/SiO₂ is 124 for micro-TS-1.

^bUnless particularly stated, the MW of PAM is 8000000-15000000.

Table S2. Textural properties of synthesized TS-1 samples.

	Si/Ti ^a	S _{BET} (m ² g ⁻¹) ^b	S _{micro} (m ² g ⁻¹) ^c	S _{ext} (m ² g ⁻¹) ^c	V _{total} (cm ³ g ⁻¹) ^d	V _{micro} (cm ³ g ⁻¹) ^e	V _{meso} (cm ³ g ⁻¹) ^f
P-0-80-120	107	389	276	112	0.49	0.15	0.34
P-5-80-120	52	369	228	141	0.50	0.10	0.40
P-10-80-120	29	339	232	106	0.40	0.09	0.31
P-20-80-120	26	276	189	88	0.16	0.07	0.09

^aThe elemental compositions in the bulk were determined by ICP, ^bSurface area was calculated from the nitrogen adsorption isotherm using the BET method; ^cS_{micro} (micropore area), S_{ext} (external surface area) were calculated using the t-plot method. ^dV_{total} (total pore volume) at P/P₀ = 0.99; ^eV_{micro} (micropore volume) was calculated using the t-plot method. ^fV_{meso} (mesopore volume) = V_{total} (total pore volume) - V_{micro}.

Table S3. Si/Ti ratio of synthesized samples.^a

	Crystallization time (80 °C)	Crystallization time (120 °C)	Si/Ti
AM-10-80-120	3 h	12 h	85
P800-10-80-120	3 h	3 h	28
P1800-10-80-120	3 h	6 h	59
PEI-10-80-120	3 h	6 h	69
PDDA-10-80-120	3 h	8 h	126

^aThe elemental compositions in the bulk were determined by ICP.

Table S4. Oxidation of 1-hexene over synthesized TS-1 samples.^a

	Conv.	Sel. (%)	H₂O₂	
	Max (%)		Conv. (%)	Effic. (%)
P-0-80-120	18.3	>99	22.7	80.6
P-5-80-120	20.0	99	27.6	72.5
P-10-80-120	26.5	98	36.2	73.2
P-10-80-120-HCl	21.4	99	25.7	83.3
P-20-80-120	2.30	>99	15.2	15.1
TiO ₂	1.01	>99	18.2	5.5

^aReaction conditions: cat., 50 mg; 1-hexene, 10 mmol; H₂O₂ (35 wt%), 3.3 mmol; methanol, 8.0 g; temp., 333 K.